

# Determination of the Material Characteristics by Means of a High Speed Tensile Test – Experiments and Simulations

O. K. Demir<sup>1</sup>, O. Höhling<sup>1</sup>, D. Risch<sup>1</sup>, A. Brosius<sup>1</sup>, A. E. Tekkaya<sup>1</sup>

<sup>1</sup>*Institute of Forming Technology and Lightweight Construction (IUL) – Technische Universität Dortmund, Baroper Str. 301, 44227 Dortmund*

URL: [www.iul.eu](http://www.iul.eu)

e-mail: [koray.demir@iul.uni-dortmund.de](mailto:koray.demir@iul.uni-dortmund.de);  
[ortrun.hoehling@iul.uni-dortmund.de](mailto:ortrun.hoehling@iul.uni-dortmund.de);  
[desiree.risch@iul.uni-dortmund.de](mailto:desiree.risch@iul.uni-dortmund.de);  
[alexander.brosius@iul.uni-dortmund.de](mailto:alexander.brosius@iul.uni-dortmund.de);  
[erman.tekkaya@iul.uni-dortmund.de](mailto:erman.tekkaya@iul.uni-dortmund.de)

**ABSTRACT:** Three high speed tensile tests of the aluminum alloy AlMg3 and finite element (FE) simulations of these tests were performed. The strain rate dependency parameters for the Cowper-Symonds material model, which minimize the difference between measured and simulated displacement results, were determined. The verification of the determined parameters by means of strain distribution comparisons between an additional experiment and its simulation revealed the necessity for further consideration of the parameters.

**Keywords:** High speed tensile test, material characterisation, finite element simulation

## 1 INTRODUCTION & MOTIVATION

The enhanced formability of aluminum at high strain rates makes high speed forming processes of this material more and more attractive, which, in turn, increases the necessity for a better understanding of these processes. FE simulations are widely used for this aim; however, due to strain rate sensitivity of aluminum and its alloys at high strain rates knowledge of material data that is valid at high strain rates is essential in order to obtain accurate results in simulations.

One way to acquire this information is high speed sheet tensile testing, which is known as one of the most difficult ways of material evaluation [1] due to mechanical vibrations complicating force measurements, high inertial forces, adiabatic increase of temperature, and continuous variation of local and temporary strain and strain rate during the test [2].

In this study, an inverse engineering method was used in order to avoid these difficulties of the test with the help of FE simulations. By means of an optimization loop the material parameters of AlMg3 for the viscoplastic material model of Cowper and Symonds [3] were determined.

## 2 DESCRIPTION OF THE EXPERIMENTAL & NUMERICAL SETUP

### 2.1 Experimental Setup & Measurement Systems

The experimental setup for the analysed high speed tensile tests is presented in figure 1. The specimen is fixed with pins between the upper and lower plunger and this plunger-specimen-unit is positioned at the upper end of the acceleration pipe. The test is started by dropping the plunger-specimen-unit. In order to achieve velocities up to 25 m/s, which are higher than those realized merely by gravity (approx. 10 m/s), an additional pressure supply can be used. At the lower end of the acceleration tube the upper plunger is suddenly stopped by an anvil, while the specimen is elongated due to the continuation of the lower plunger's movement caused by inertia.

In order to determine the course of this movement, an online measurement system using the effect of shadowing a light beam is applied (see figure 2). The principle is well known from several publications in the field of high speed forming of tubes. With modern electronic components a measurement system has been designed and adapted to the current setup [5].

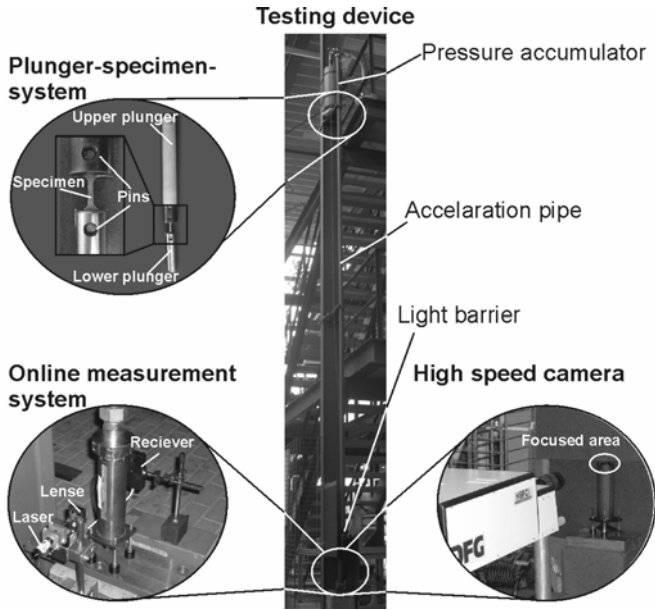


Fig. 1 Experimental setup and measurement systems

The system consists of a laser beam which is expanded to a line, parallelized by a lens, and received by a so called Position Sensitive Device (PSD). During the deformation process the lower plunger moves between laser and receiver, partly shadowing the laser light so that the quantity of light changes directly proportional to the displacement of the lower plunger.

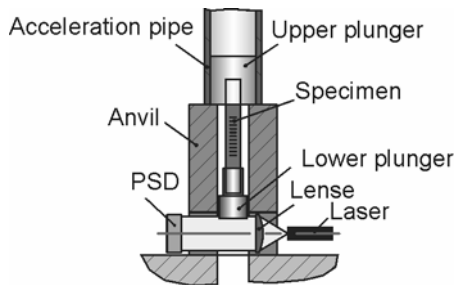


Fig. 2 Principle of Laser-PSD

An additional measurement facility (see figure 1), which is adapted to the testing device, is the high speed camera HSFC.pro (company PCO, Germany). This camera is able to take eight pictures within a variable time interval reaching from a tenth of a microsecond to seconds. Figure 6 shows a series of four pictures from the whole sequence. Furthermore, a stochastic pattern can be recognized which is necessary in order to do a strain analysis with the Aramis system developed by the GOM company [6]. The last adapted measurement device is a light barrier which is integrated in the acceleration pipe in order to trigger the high speed camera. Additionally, using again the effect of shadowing a light beam, it is possible to determine the fall velocity of the plunger-specimen-unit. The experimental data of all

adapted measurement devices will be the input as well as reference for the numerical analysis.

## 2.2 Numerical Setup

The FE simulations were performed using the dynamic explicit three dimensional solver of the commercial code LS-DYNA, employing brick-shaped elements with eight nodes, single integration point, and hourglass control.

The necessity for the dynamic calculation arises from the fact that the transit times for the stress waves travelling along the specimen are long with respect to the duration of the application of tensile forces. During the experiments the fracture of the specimen occurs in certain cases after approx. 300  $\mu$ s, while a mechanical wave travels back and forth along the specimen in 24  $\mu$ s, which means that a stress wave moves back and forth only 12 times during the whole test. This prevents the equilibrium of forces in the specimen from evolving and makes a static assumption useless.

The assumption of linear elastic material behaviour was made for the pins, while the viscoplastic constitutive model developed by Cowper and Symonds was used for the plastic deformation of the specimen, neglecting the effect of adiabatic heating. This model is selected based on the low number of variables, which means a reduced number of simulations during the optimization loops. The application of the Cowper-Symonds model in LS-DYNA requires the elastic constants and the quasi-static (q-s) flow curve of the material and scales the given flow stress values with a factor calculated by eq. (1) given below:

$$\text{Scale factor} = 1 + \left( \frac{\dot{\epsilon}}{C} \right)^{1/p}, \quad (1)$$

where  $\dot{\epsilon}$  is the strain rate and  $C$  and  $p$  are the Cowper-Symonds strain rate parameters. The q-s flow curve of AlMg3 for the simulations was obtained by a conventional tension test.

A representative mesh of the specimen and the dimensions of the model can be seen in figure 3. 46,000 elements have been used for the numerical model of the specimen. The front pin is attached to a point mass, which represents the lower plunger. While the whole model (specimen, pins, and the plunger) has a certain initial velocity in  $x$ -direction, the nodes in the front region of the back pin are constrained in  $x$ -direction, which represents the impact between the back pin and the plunger that occurs

when the plunger stops suddenly.

In order to simulate a given experiment, the velocity of the plunger-specimen unit just before the impact needs to be measured. This velocity is transferred to the FE simulation as an initial condition. The outputs of the simulation and experiment can be compared considering the displacement course of the lower plunger.

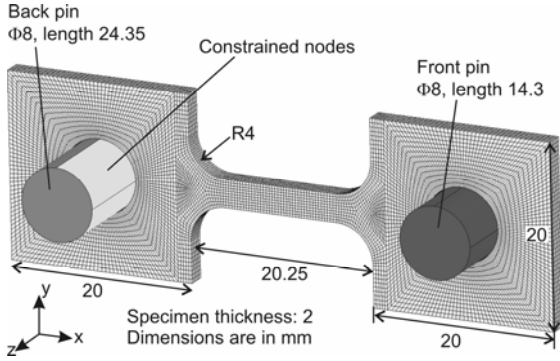


Fig. 3 FE model

### 2.3 Determination of the Material Parameters

In order to determine the  $C$ - $p$  couple equating the displacement results of a simulation to the corresponding experiment, first, two simulations were performed with two initial guesses of the  $C$ - $p$  couple. The following guesses were calculated by a simplex-based optimization algorithm developed by Nelder and Mead [4] until the objective function given below is minimized:

$$f(C, p) = \sum (u_{\text{exp}} \cdot \dot{u}_{\text{exp}} - u_{\text{sim}} \cdot \dot{u}_{\text{sim}})^2, \quad (2)$$

where  $u$  and  $\dot{u}$  represent the displacement and velocity of the lower plunger and subscripts “exp” and “sim” stand for experiment and simulation, respectively. The objective function was evaluated by taking only experimental data until fracture into account.

There can be more than one  $C$ - $p$  couple that makes a simulation result coincident with the corresponding measurement. Furthermore, the  $C$ - $p$  couple determined for an experiment depends on the initial guesses supplied by the user and it is not necessarily valid for other experiments performed at different velocities. Here, our aim was to determine a  $C$ - $p$  couple valid for all experiments at hand. The reliability of the determined couple is directly proportional to the number of experiment-simulation pairs taken into account during the optimization process. For this study, three experiments were performed at: 11.4 m/s, 15.9 m/s, and 22.6 m/s.

## 3 RESULTS

### 3.1 Course of Plunger Displacement

Figure 4 reveals the experiment results and simulation results when  $C=p=0$  (q-s flow curve is used) and when  $C=850$  and  $p=0.03$ .

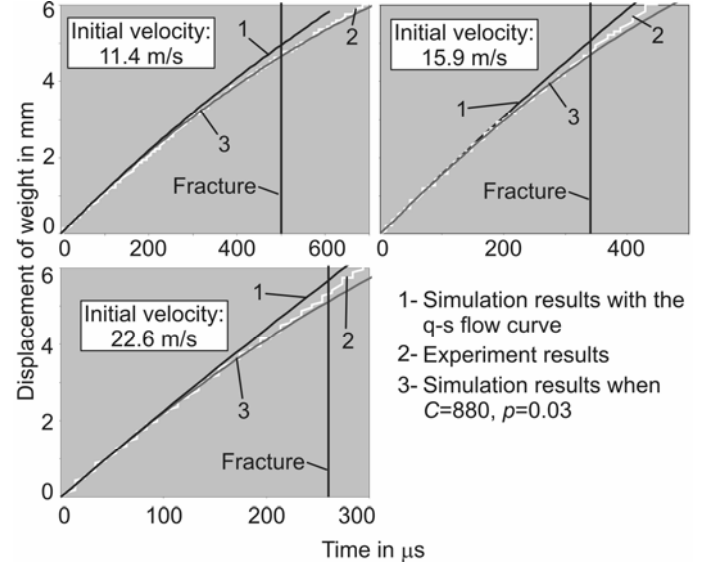


Fig. 4 Measured and calculated plunger displacement courses

When the tests were simulated using the q-s flow curve of the material, the simulations overestimated the measured displacements of the lower plunger severely, as expected. The utilization of the mentioned  $C$ - $p$  couple reduced the maximum error values until fracture to 5.9%, 1.9%, and 4.3% for the cases of 11.4 m/s, 15.9 m/s, and 22.6 m/s initial velocities, respectively.

As can be seen in figure 5, with these parameters the material gains a very strong strain rate dependency. The parameter  $p$  decides the sensitivity of the scale factor to strain rate. A very small value, as the one found, leads to an extreme sensitivity and very large scale factors above a strain rate of  $880 \text{ s}^{-1}$ . The importance of the factor  $C$  arises at this point: it determines this critical strain rate value, above which the calculated scale factors are very large. Hence, for small values of  $p$  the scale factor is also very sensitive to  $C$ , which is another disadvantage of the determined parameter couple.

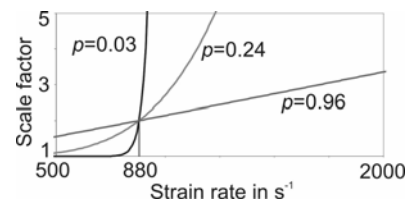


Fig. 5 Scale factor with respect to strain rate and  $p$

### 3.2 Course of Strain Distribution

In order to validate the determined material parameters, an additional experiment with a velocity of 9.2 m/s, which is outside the range of the other three velocities, was carried out and eight pictures were taken using the high speed camera. Four representative photos are given in figure 6.

The elongation at fracture measured after the experiment was 4 mm. Since the high speed camera and the displacement measurement setup cannot be used simultaneously the according time period must be approximated. According to an extrapolation of previous experiment results, a duration of 600  $\mu\text{s}$  was estimated. Thus, the time at figure 6c was assumed to be 600  $\mu\text{s}$  due to the occurring fracture. Knowing the time period between two photos being 100  $\mu\text{s}$ , the time for all the photos can be deduced.

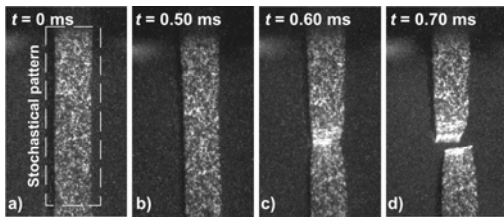


Fig. 6 Photos from a high speed tensile test. a) initial state, b) elongation, c) fracture, and d) the state after the fracture

Next, the strain distribution on the surface of the specimen along the centreline was analysed using the Aramis system and the results were compared to the simulations. Figure 7 shows the comparison.

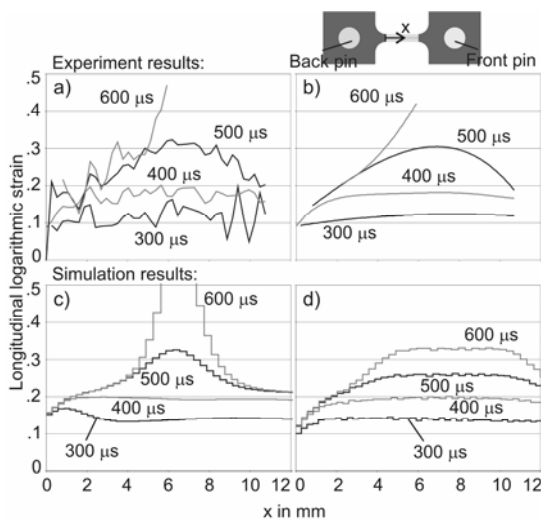


Fig. 7 Strain distribution courses. a) experiment results, b) trendlines of experiment results, c) simulation results ( $C=p=0$ ), d) simulation results ( $C=880, p=0.03$ )

Applying the parameters prevents strain localization that takes place at  $t=300 \mu\text{s}$  around  $x=1$ , and later at

$t=500 \mu\text{s}$  in the necking region. These changes make the simulation results resemble the experimental results qualitatively, but the strain evolution, obvious in the experiment data, cannot be acquired in the simulation.

This can be explained by errors in measuring the initial specimen velocity, measuring strains, or approximating the moments, when the photos were taken. It might also indicate that the Cowper-Symonds model or the determined parameters are unsuitable for modelling the behaviour of AlMg3.

### 4 SUMMARY

A combined experimental and numerical approach for determining the material behaviour of AlMg3 at high strain rates was tested. Therefore, a high speed tensile test including several measurement systems was realized. FE simulations were carried out in order to find the Cowper-Symonds material constants by means of an inverse analysis. The determined constants are pretty successful in predicting experimental displacements, but the strain results need more consideration. Applying the same methodology with more experiments, or verifying the used material model or measurement techniques are conceivable alternatives for further research.

### ACKNOWLEDGEMENTS

The authors would like to thank the German Research Foundation (DFG) for its financial support of the work reported here, acquired within the scope of Research Unit FOR 443.

### REFERENCES

1. P. Larour, A. Rusinek, J.R. Klepaczko and W. Bleck, 'Effects of Strain Rate and Identification of Material Constants for Three Automotive Steels', *Steel Research Int.*, 78, (2007) 348-358
2. M. Kleiner and A. Brosius, 'Determination of Flow Curves at High Strain Rates using the Electromagnetic Forming Process and an Iterative Finite Element Simulation Scheme', *CIRP Annals - Manufacturing Technology*, 55, (2006) 267-270
3. P.S. Symonds, 'Survey of Methods of Analysis for plastic deformation of structures under dynamic loading', Technical Report, Brown University, 1967
4. J.A. Nelder, R. Mead, 'A Simplex Method for Function Minimization', *Computer Journal*, 7, (1965) 308-313
5. M. Badelt, C. Beerwald, A. Brosius and M. Kleiner, Process Analysis of Electromagnetic Sheet Metal Forming by Online-Measurement and Finite Element Simulation. Proc. of the 6th ESAFORM, 2003, 123-126
6. www.gom.com